Numerical investigation on high power mid-infrared supercontinuum fiber lasers pumped at 3 μm

Chen Wei,[1,2] Xiushan Zhu,[2,*] Robert A. Norwood,[2] Feng Song,[1] and N. Peyghambarian[2]

[1]*Photonics Center, College of Physical Sciences, Nankai University, Weijin Road 94, Tianjin, 300071, China*
[2]*College of Optical Sciences, University of Arizona, 1630 E. University Blvd., Tucson, AZ, 85721, USA*
[3]*These author contributed equally.*
[4]*fsong@nankai.edu.cn*
[*]*xszhu@ email.arizona.edu*

Abstract: High power mid-infrared (mid-IR) supercontinuum (SC) laser sources in the 3-12 μm region are of great interest for a variety of applications in many fields. Although various mid-IR SC laser sources have been proposed and investigated experimentally and theoretically in the past several years, power scaling of mid-IR SC lasers beyond 3 μm with infrared edges extending beyond 7 μm are still challenges because the wavelengths of most previously used pump sources are below 2 μm. These problems can be solved with the recent development of mode-locked fiber lasers at 3 μm. In this paper, high power mid-IR SC laser sources based on dispersion engineered tellurite and chalcogenide fibers and pumped by ultrafast lasers at 3 μm are proposed and investigated. Our simulation results show that, when a W-type tellurite fiber with a zero dispersion wavelength (ZDW) of 2.7 μm is pumped at 2.78 μm, the power proportion of the SC laser beyond 3 μm can exceed 40% and the attainable SC output power of the proposed solid-cladding tellurite fiber is one order of magnitude higher than that of existing microstructured tellurite fibers. Our calculation also predicts that a very promising super-broadband mid-IR SC fiber laser source covering two atmospheric windows and molecules' "fingerprint" region can be obtained with a microstructured As_2Se_3 chalcogenide fiber pumped at 2.78 μm.

OCIS codes: (060.2280) Fiber design and fabrication; (060.2390) Fiber optics, infrared; (060.4370) Nonlinear optics, fibers; (060.7140) Ultrafast processes in fibers; (320.6629) Supercontinuum generation; (060.5295) Photonic crystal fibers; (060.4005) Microstructured fibers.

References and links

1. K.-D. F. Büchter, H. Herrmann, C. Langrock, M. M. Fejer, and W. Sohler, "All-optical Ti:PPLN wavelength conversion modules for free-space optical transmission links in the mid-infrared," Opt. Lett. **34**(4), 470–472 (2009).
2. S. T. Sanders, "Wavelength-agile fiber laser using group-velocity dispersion of pulsed super-continua and application to broadband absorption spectroscopy," Appl. Phys. B **75**(6–7), 799–802 (2002).
3. M. G. Allen, "Diode laser absorption sensors for gas-dynamic and combustion flows," Meas. Sci. Technol. **9**(4), 545–562 (1998).
4. http://www.nktphotonics.com/
5. K. Kikuchi, K. Taira, and N. Sugimoto, "Highly nonlinear bismuth oxide-based glass fibers for all-optical signal processing," Electron. Lett. **38**(4), 166–167 (2002).
6. J. Gopinath, H. Shen, H. Sotobayashi, E. Ippen, T. Hasegawa, T. Nagashima, and N. Sugimoto, "Highly nonlinear bismuth-oxide fiber for smooth supercontinuum generation at 1.5 microm," Opt. Express **12**(23), 5697–5702 (2004).
7. G. Brambilla, F. Koizumi, V. Finazzi, and D. J. Richardson, "Supercontinuum generation in tapered bismuth silicate fibres," Electron. Lett. **41**(14), 795–797 (2005).

8. J. T. Gopinath, H. M. Shen, H. Sotobayashi, E. P. Ippen, T. Hasegawa, T. Nagashima, and N. Sugimoto, "Highly nonlinear bismuth-oxide fiber for supercontinuum generation and femtosecond pulse compression," J. Lightwave Technol. **23**(11), 3591–3596 (2005).
9. R. Buczynski, H. T. Bookey, D. Pysz, R. Stepien, I. Kujawa, J. E. McCarthy, A. J. Waddie, A. K. Kar, and M. R. Taghizadeh, "Supercontinuum generation up to 2.5 μm in photonic crystal fiber made of lead-bismuth-galate glass," Laser Phys. Lett. **7**(9), 666–672 (2010).
10. J. H. V. Price, T. M. Monro, H. Ebendorff-Heidepriem, F. Poletti, P. Horak, V. Finazzi, J. Y. Y. Leong, P. Petropoulos, J. C. Flanagan, G. Brambilla, X. Feng, and D. J. Richardson, "Mid-IR supercontinuum generation from nonsilica microstructured optical fibers," IEEE J. Sel. Top. Quantum Electron. **13**(3), 738–749 (2007).
11. X. Zhu and N. Peyghambarian, "High-power ZBLAN glass fiber lasers: review and prospect," Adv. Optoelectron. **2010**, 501956 (2010).
12. C. Xia, Z. Xu, M. N. Islam, F. L. Terry, Jr., M. J. Freeman, A. Zakel, and J. Mauricio, "10.5 W time-averaged power mid-IR supercontinuum generation extending beyond 4 μm with direct pulse pattern modulation," IEEE J. Sel. Top. Quantum Electron. **15**(2), 422–434 (2009).
13. G. Qin, X. Yan, C. Kito, M. Liao, C. Chaudhari, T. Suzuki, and Y. Ohishi, "Ultrabroadband supercontinuum generation from ultraviolet to 6.28 μm in a fluoride fiber," Appl. Phys. Lett. **95**(16), 161103 (2009).
14. J. Swiderski, M. Michalska, and G. Maze, "Mid-IR supercontinuum generation in a ZBLAN fiber pumped by a gain-switched mode-locked Tm-doped fiber laser and amplifier system," Opt. Express **21**(7), 7851–7857 (2013).
15. J. S. Wang, E. M. Vogel, and E. Snitzer, "Tellurite glass: new candidate for fiber devices," Opt. Mater. **3**(3), 187–203 (1994).
16. G. Ghosh, "Sellmeier coefficients and chromatic dispersions for some tellurite glasses," J. Am. Ceram. Soc. **78**(10), 2828–2830 (1995).
17. P. Domachuk, N. A. Wolchover, M. Cronin-Golomb, A. Wang, A. K. George, C. M. B. Cordeiro, J. C. Knight, and F. G. Omenetto, "Over 4000 nm bandwidth of mid-IR supercontinuum generation in sub-centimeter segments of highly nonlinear tellurite PCFs," Opt. Express **16**(10), 7161–7168 (2008).
18. I. Savelii, J. C. Jules, G. Gadret, B. Kibler, J. Fatome, M. El-Amraoui, N. Manikandan, X. Zheng, F. Désévédavy, J. M. Dudley, J. Troles, L. Brilland, G. Renversez, and F. Smektala, "Suspended core tellurite glass optical fibers for infrared supercontinuum generation," Opt. Mater. **33**(11), 1661–1666 (2011).
19. M. Liao, C. Chaudhari, G. Qin, X. Yan, T. Suzuki, and Y. Ohishi, "Tellurite microstructure fibers with small hexagonal core for supercontinuum generation," Opt. Express **17**(14), 12174–12182 (2009).
20. M. Liao, X. Yan, G. Qin, C. Chaudhari, T. Suzuki, and Y. Ohishi, "A highly non-linear tellurite microstructure fiber with multi-ring holes for supercontinuum generation," Opt. Express **17**(18), 15481–15490 (2009).
21. G. Qin, M. Liao, C. Chaudhari, X. Yan, C. Kito, T. Suzuki, and Y. Ohishi, "Second and third harmonics and flattened supercontinuum generation in tellurite microstructured fibers," Opt. Lett. **35**(1), 58–60 (2010).
22. G. Qin, X. Yan, C. Kito, M. Liao, T. Suzuki, A. Mori, and Y. Ohishi, "Zero-dispersion-wavelength-decreasing tellurite microstructured fiber for wide and flattened supercontinuum generation," Opt. Lett. **35**(2), 136–138 (2010).
23. M. Liao, X. Yan, W. Gao, Z. Duan, G. Qin, T. Suzuki, and Y. Ohishi, "Five-order SRSs and supercontinuum generation from a tapered tellurite microstructured fiber with longitudinally varying dispersion," Opt. Express **19**(16), 15389–15396 (2011).
24. G. Qin, X. Yan, C. Kito, M. Liao, T. Suzuki, A. Mori, and Y. Ohishi, "Highly nonlinear tellurite microstructured fibers for broadband wavelength conversion and flattened supercontinuum generation," J. Appl. Phys. **107**(4), 043108 (2010).
25. G. Qin, X. Yan, M. Liao, A. Mori, T. Suzuki, and Y. Ohishi, "Wideband supercontinuum generation in tapered tellurite microstructured fibers," Laser Phys. **21**(6), 1115–1121 (2011).
26. M. Liao, W. Gao, Z. Duan, X. Yan, T. Suzuki, and Y. Ohishi, "Supercontinuum generation in short tellurite microstructured fibers pumped by a quasi-cw laser," Opt. Lett. **37**(11), 2127–2129 (2012).
27. C. Wei, X. Zhu, R. A. Norwood, and N. Peyghambarian, "Passively continuous-wave mode-locked Er($^{3+}$)-doped ZBLAN fiber laser at 2.8 μm," Opt. Lett. **37**(18), 3849–3851 (2012).
28. J. Li, D. D. Hudson, Y. Liu, and S. D. Jackson, "Efficient 2.87 μm fiber laser passively switched using a semiconductor saturable absorber mirror," Opt. Lett. **37**(18), 3747–3749 (2012).
29. J. Hu, C. R. Menyuk, L. B. Shaw, J. S. Sanghera, and I. D. Aggarwal, "Maximizing the bandwidth of supercontinuum generation in As_2Se_3 chalcogenide fibers," Opt. Express **18**(7), 6722–6739 (2010).
30. D. I. Yeom, E. C. Mägi, M. R. Lamont, M. A. Roelens, L. Fu, and B. J. Eggleton, "Low-threshold supercontinuum generation in highly nonlinear chalcogenide nanowires," Opt. Lett. **33**(7), 660–662 (2008).
31. M. R. Lamont, B. Luther-Davies, D. Y. Choi, S. Madden, and B. J. Eggleton, "Supercontinuum generation in dispersion engineered highly nonlinear (γ = 10 /W/m) As_2S_3) chalcogenide planar waveguide," Opt. Express **16**(19), 14938–14944 (2008).
32. M. El-Amraoui, J. Fatome, J. C. Jules, B. Kibler, G. Gadret, C. Fortier, F. Smektala, I. Skripatchev, C. F. Polacchini, Y. Messaddeq, J. Troles, L. Brilland, M. Szpulak, and G. Renversez, "Strong infrared spectral broadening in low-loss As-S chalcogenide suspended core microstructured optical fibers," Opt. Express **18**(5), 4547–4556 (2010).
33. J. S. Sanghera, I. D. Aggarwal, L. B. Shaw, C. M. Florea, P. Pureza, V. Q. Nguyen, and F. Kung, "Nonlinear properties of chalcogenide glass fibers," J. Optoelectron. Adv. Mater. **8**, 2148–2155 (2006).

#198149 - $15.00 USD Received 23 Sep 2013; revised 12 Nov 2013; accepted 12 Nov 2013; published 21 Nov 2013

34. A. Marandi, C. W. Rudy, V. G. Plotnichenko, E. M. Dianov, K. L. Vodopyanov, and R. L. Byer, "Mid-infrared supercontinuum generation in tapered chalcogenide fiber for producing octave-spanning frequency comb around 3 μm," Opt. Express **20**(22), 24218–24225 (2012).
35. P. Klocek, *Handbook of Infrared Optical Materials* (Marcel Dekker, 1991).
36. G. Genty, S. Coen, and J. M. Dudley, "Fiber supercontinuum sources (Invited)," J. Opt. Soc. Am. B **24**(8), 1771–1785 (2007).
37. X. Yan, G. Qin, M. Liao, T. Suzuki, and Y. Ohishi, "Transient Raman response and soliton self-frequency shift in tellurite microstructured fiber," J. Appl. Phys. **108**(12), 123110 (2010).
38. A. Ben-Salem, R. Cherif, and M. Zghal, "Raman response of a highly nonlinear As_2Se_3-based chalcogenide photonic crystal fiber," Proc. PIERS, 1256–1260, Marrakesh, Morocco (2011).
39. T. M. Monro and H. Ebendorff-Heidepriem, "Progress in microstructured optical fibers," Annu. Rev. Mater. Res. **36**(1), 467–495 (2006).
40. K. Richardson, D. Krol, and K. Hirao, "Glasses for photonic applications," Int. J. Appl. Glass. Sci. **1**(1), 74–86 (2010).
41. http://www.npphotonics.com/
42. J. M. Dudley, G. Gentry, and S. Coen, "Supercontinuum generation in photonic crystal fiber," Rev. Mod. Phys. **78**(4), 1135–1184 (2006).
43. "FIMMWAVE Version 4.06," Photon Design, Dec. 2002.
44. R. Stegeman, L. Jankovic, H. Kim, C. Rivero, G. Stegeman, K. Richardson, P. Delfyett, Y. Guo, A. Schulte, and T. Cardinal, "Tellurite glasses with peak absolute Raman gain coefficients up to 30 times that of fused silica," Opt. Lett. **28**(13), 1126–1128 (2003).
45. R. Cherif, A. Ben Salem, M. Zghal, P. Besnard, T. Chartier, L. Brilland, and J. Troles, "Highly nonlinear As_2Se_3-based chalcogenide photonic crystal fiber for mid-infrared supercontinuum generation," Opt. Eng. **49**, 095002 (2010).
46. http://www.coractive.com/
47. C. Xia, M. Kumar, M.-Y. Cheng, R. S. Hegde, M. N. Islam, A. Galvanauskas, H. G. Winful, F. L. Terry, Jr., M. J. Freeman, M. Poulain, and G. Mazé, "Power scalable mid-infrared supercontinuum generation in ZBLAN fluoride fibers with up to 1.3 watts time-averaged power," Opt. Express **15**(3), 865–871 (2007).
48. J. S. Sanghera and I. D. Aggarwal, "Active and passive chalcogenide glass optical fibers for IR applications: a review," J. Non-Cryst. Solids **256–257**, 6–16 (1999).
49. N. Granzow, S. P. Stark, M. A. Schmidt, A. S. Tverjanovich, L. Wondraczek, and P. S. Russell, "Supercontinuum generation in chalcogenide-silica step-index fibers," Opt. Express **19**(21), 21003–21010 (2011).

1. Introduction

High power broadband laser sources in the mid-infrared (mid-IR) wavelength range have attracted increasing attention in recent years because of the extensive applications of mid-IR light in military, astronomy, remote sensing and ranging, explosive and chemical detection [1], spectroscopy [2], and biomedical surgery [3]. Supercontinuum (SC) generation, in which the spectrum of a laser undergoes substantial spectral broadening through the interplay of nonlinear effects including self-phase modulation (SPM), cross phase modulation, four wave mixing, Raman scattering, and modulation instability, has been widely investigated to obtain ultra-broadband light sources with extremely high brightness. SC generation has been observed in a wide variety of nonlinear media including organic and inorganic liquids, gases, bulk solids, and waveguides. Optical fibers have been considered as an inherently excellent candidate for SC generation because they can provide a significant length for nonlinear interaction. The maturity of microstructured silica glass fibers, whose core and cladding construction can be tailored to provide engineered dispersions and highly confined single-mode cores, has greatly benefited SC generation. SC sources with spectra spanning from 0.4 μm to ~2.4 μm generated in a microstructured silica fiber have been commercially available for several years [4]. However, silica fiber has two main limitations for mid-IR SC generation: low nonlinearity (nonlinear refractive index $n_2 = 2.2 \times 10^{-20}$ m^2/W) and short IR transmission edge (< 3 μm). Some non-silica glass fibers including ZBLAN (ZrF_4-BaF_2-LaF_3-AlF_3-NaF), bismuth, tellurite, and chalcogenide, can overcome one or both constraints and have been considered as promising candidates for mid-IR SC generation. All these glasses have high transmission in the mid-IR or even long-wave IR region and have nonlinearities comparable to or much higher than that of silica. Mid-IR SC generation in fibers based on these glasses has been extensively investigated experimentally and theoretically in the last several years. Because of its high nonlinearity (n_2 = 3.2 × 10^{-19} m^2/W [5]) and broad IR transparency, bismuth fiber has been proposed for mid-IR SC generation [6–9]. Price et al. [10] have theoretically demonstrated that it is possible to achieve a SC spanning from 2 to 5 μm using a bismuth glass PCF. However, the power percentage of the SC in the 3-5 μm wavelength range was still less than 5%. Moreover, there is still no experimental demonstration of mid-IR SC generation based on bismuth glass fibers yet. To date most mid-IR SC generation was achieved in ZBLAN, tellurite, and chalcogenide fibers.

ZBLAN glass is the most stable heavy metal fluoride glass and an excellent host for rare-earth ions; ZBLAN has been used for nearly 40 years and rare-earth doped ZBLAN fibers have been used to develop a variety of ultraviolet, visible, and infrared lasers that cannot be achieved in silica fibers [11]. Because of its low intrinsic loss and wide transparency window, ZBLAN fiber has been used to generate SC spanning from the visible to mid-IR [12,13]. However, ZBLAN has an n_2 comparable to silica and hence a long optical fiber has to be used to achieve high conversion efficiency and high flatness SC sources. Moreover, since the zero dispersion wavelength (ZDW) of ZBLAN is 1.6 μm, a pump wavelength close to 1.6 μm is generally required for broadband SC generation, which results in relatively low power proportion of mid-IR in the SC. For instance, a 10 W SC laser source spanning over ~0.8-4 μm based on ZBLAN fiber has been reported by Xia, et al. [12]. However, most of the ZBLAN laser power has a wavelength below 3 μm and the IR edge is only 4 μm. Qin et al. have achieved SC light expanding from 0.35 to 6.28 μm in a centimeter-long ZBLAN fiber pumped by a 1.45 μm femtosecond laser [13]. But the output power was at the level of mW and the total power beyond 3 μm in the mid-IR region was < 5 mW. Most recently, J. Swiderski et al. demonstrated SC generation with output power of 125 mW for wavelengths above 3 μm. However, the IR edge was not beyond 4 μm [14]. Therefore, ZBLAN fiber is not an ideal candidate for high power mid-IR SC generation in the 3-12 μm wavelength region. Because tellurite has much higher robustness and chalcogenide has a much longer IR edge (~12 μm) than ZBLAN glass and, more importantly, both of them have higher n_2 than ZBLAN glass by at least one order of magnitude, tellurite and chalcogenide fibers have been considered as promising candidates for high power mid-IR SC laser sources with high spectral power densities in the 3-5 μm and 8-12 μm atmospheric windows and molecular "fingerprint" region.

Tellurite glass has been extensively used as a low phonon energy oxide glass in nonlinear photonic devices due to its broad IR transmission and large nonlinearity. Compared to other mid-IR transmitting glasses such as ZBLAN and chalcogenide glasses, tellurite glass exhibits higher robustness, stronger corrosion resistance, and better thermal stability [15]. In addition, they are non-hygroscopic, which allows storage in ambient air without degradation and makes tellurite glass devices require less protection. In recent years, experimental and theoretical investigations on mid-IR SC generation in tellurite fibers have attracted increasing interest. Because the ZDW of tellurite glass is ~2.3 μm [16], microstructured, tapered or combination of both structured tellurite fibers with tailored ZDWs close to the wavelengths of readily available near IR pump sources have been employed in previous works [17–26]. However, the mid-IR power proportion of these tellurite fiber SC laser sources is as small as that of ZBLAN fiber SC laser sources because they are all pumped in the near-IR. Moreover, the small effective core areas of these microstructured or tapered tellurite fibers easily suffer from breakdown damage thereby constraining the power scaling of these SC laser sources. For instance, Domachuk et al. have reported an SC laser source with its IR edge extending to 4.5 μm using an 8 mm microstructured tellurite PCF [17]. This PCF had a ZDW of 1380 nm, which enables the pump pulse (1559 nm) to propagate in the region of anomalous dispersion and thus broadening the laser spectrum significantly through soliton fission and Raman scattering. A spectral range of over two octaves was obtained (789-4870 nm). However, the average power of the SC laser source was only 70 mW and most of power was confined to the wavelength region below 2 μm. In addition, the effective area of the fiber mode was only 1.7

μm^2 and power scaling of this SC fiber laser source will be highly limited by the damage of the fiber end facet under high power pumping. In order to obtain tens or hundreds of watts mid-IR SC laser sources, solid-cladding large core tellurite fibers should be promising candidates. However, it is hard to obtain ultra-broadband SC in a conventional step-indexed tellurite fiber because substantial spectral broadening generally occurs in an optical fiber pumped at a wavelength close to the ZDW, while most current readily available ultrafast laser sources have wavelengths much shorter than the ZDW (2.3 μm) of tellurite glass. Recently, we have demonstrated a mode-locked Er^{3+}-doped ZBLAN fiber laser at 2.78 μm with a pulse duration of 19 ps and an average power of 51 mW [27]. Partially mode-locked 2.87 μm pulses with a duration of 24 ps and an average power of 132 mW from a passively switched Ho^{3+}/Pr^{3+} co-doped ZBLAN fiber laser have also been reported by Li et al. [28]. Further scaling of the average power and reduction of the pulse duration are expected with the incorporation of power amplifiers and proper dispersion compensation in the cavity, respectively. Both aforementioned laser sources are promising pump sources for high power mid-IR SC generation in tellurite fibers since their wavelengths are in the anomalous dispersion region where the generation and control of solitons are easier and most nonlinear effects are of significance. Therefore, pumping a tellurite fiber with an ultrafast fiber laser at 3 μm is a promising approach to obtain a high power mid-IR SC laser source with high spectral power density in the 3-5 μm atmospheric window.

Chalcogenide glass is a member of the group of non-oxide glass that contains one or more of the chalcogen elements: S, Se or Te has very high nonlinearity ($n_2 = 1.5 \times 10^{-17}$ m^2/W [29], hundreds of times higher than silica) and excellent IR transmission (up to 12 μm) and has been extensively used to fabricate various mid-IR photonic devices. Although chalcogenide fiber is generally less robust than tellurite or even ZBLAN fiber, chalcogenide glass fiber has been considered as the most promising nonlinear medium for the generation of mid-IR SC spanning over the 3-5 μm and 8-10 μm two atmospheric windows and covering most of the molecular “fingerprint” spectral region. Several experimental and theoretical investigations on SC generation in chalcogenide fibers were reported in recent years. However, most of these chalcogenide waveguide or fiber SC laser sources have IR edges below 3 μm and low average output power [30–34] because the pump wavelength is below 2 μm and the damage threshold of chalcogenide fiber is relatively low. In order to achieve a true mid-IR SC, pump sources beyond 2 μm have been used most recently. A mid-IR SC spanning 2.1-3.4 μm has been demonstrated with As_2S_3 and As_2Se_3 fibers and an As_2Se_3 PCF pumped at 2.5 μm [33]. SC generation with a bandwidth from 2.2 to 5 μm was also obtained in a tapered As_2S_3 fiber pumped at 3.1 μm [34]. However, the bandwidths of these mid-IR SC laser sources are still very narrow compared to the ultra-broad transmission bandwidths of chalcogenide fibers. Since the promise of mid-IR SC generation in chalcogenide fiber has not been exhibited in previous work, here we propose to generate the SC with IR edge up to 12 μm by pumping a chalcogenide PCF with an ultrafast fiber laser at 3 μm. Because the ZDW of most chalcogenide glasses is around 5 μm [35], it will be easier to tailor a chalcogenide fiber to shift its ZDW to 3 μm than to 1, 1.5 or 1.9 um, where Yb^{3+}-, Er^{3+}-, and Tm^{3+}- ultrafast silica fiber lasers are available. On the other hand, because the chalcogenide PCF with ZDW of 3 μm generally has a much larger effective area than conventional tapered fibers and PCFs with ZDW below 2 μm, our chalcogenide PCF can handle much higher pump power and consequently be used to generate more powerful mid-IR SC.

In this paper, we present theoretical investigations of mid-IR SC generation in a W-type tellurite fiber and a chalcogenide PCF pumped at 2.78 μm. Propagation and evolution of the 2.78 μm pulses in the tellurite and chalcogenide fibers were calculated by solving the generalized nonlinear Schrödinger equation (GNLSE). SC generation at different pump conditions and corresponding nonlinear effects have been systematically investigated and analyzed. Due to their large core sizes, the proposed tellurite and chalcogenide fibers show significant promise for power scaling. Simulation results show that several kW mid-IR SC with 40% of the light beyond 3 μm can be obtained in a “W” type tellurite fiber and tens of watt mid-IR SC spanning over 2-12 μm can be generated in a chalcogenide PCF.

2. Simulation method

As a general numerical approach to study SC generation, pulse evolution inside tellurite and chalcogenide fibers were calculated by solving the GNLSE [36]:

$$\frac{\partial A(z,t)}{\partial z} = -\frac{\alpha}{2}A(z,t) + \sum_{m\geq 2}\frac{i^{m+1}}{m!}\beta_m\frac{\partial^m A(z,t)}{\partial t^m} + i\gamma\left(1+\frac{i}{\omega_0}\frac{\partial}{\partial t}\right)\times\left(A(z,t)\int_{-\infty}^{+\infty}R(t')\left|A(z,t-t')\right|^2 dt'\right) \quad (1)$$

where $A(z, t)$ is the electric field envelope, α is the loss coefficient, the terms β_m are the various dispersion coefficients in the Taylor series expansion of the propagation constant β at the central frequency ω_0. The nonlinear coefficient γ is given by:

$$\gamma = n_2\omega_0/(cA_{eff}) \quad (2)$$

where c is the speed of light, and A_{eff} is the fiber’s effective area. The response function $R(t)$, which includes both electronic and vibrational Raman contributions, is given by:

$$R(t) = (1-f_R)\delta(t) + f_R h_R(t) \quad (3)$$

The three terms on the right-hand side of Eq. (1) describe the linear loss, dispersion effect, and nonlinear effects, respectively. The GNLSE was numerically solved by the split-step Fourier method. We assume that the input signals are hyperbolic-secant pulses in the simulation. The Raman response functions of tellurite and chalcogenide fibers are the same as those used in [37] and [38], respectively.

3. Mid-IR SC generation in tellurite fiber

Tellurite (i.e., tellurium dioxide TeO_2 based) glasses offer excellent optical transparency in the wavelength range of 0.5-5 μm, and also have the lowest phonon energy among oxide glasses [15,39,40]. Tellurite glasses have a high nonlinear refractive index of 5.9×10^{-19} m^2/W [19]. The combination of low phonon energy and high nonlinearity make the tellurite glass fibers uniquely suitable for nonlinear applications such as SC generation in the mid-IR region. Moreover, tellurite fibers have shown a mechanical robustness of > 60 kpsi and excellent resistance to moisture exposure. Therefore, tellurite fibers are ideal media for high power mid-IR SC generation.

3.1 Mid-IR SC generation in conventional tellurite fiber

Although tellurite fiber has excellent features for high power mid-IR SC generation, it is still not easy to produce ultra-broad SC in a conventional tellurite fiber because its ZDW is ~2.3 μm [16], and currently there are no ultrafast fiber laser sources or other diode-pumped solid-state laser sources readily available at this wavelength. The most suitable pump sources are the 2 μm Tm^{3+}-doped fiber laser and ~3 μm Er^{3+} or Ho^{3+} -doped ZBLAN fiber laser. Here, we compare the SC spectra generated in conventional tellurite fiber pumping at 2 μm and 2.78 μm. The Raman gain used in our simulation was the same as that shown in Fig. 1 in [37]. The fiber had a core diameter of 8 μm and numerical aperture (NA) of 0.2. The fiber length was set to be 60 cm. Figure 1 shows the spectra of SC generated in the tellurite fiber pumped by 800 fs pulses with a peak power of 12 kW at 2 μm and 2.78 μm, respectively. The red dash-dot curve shows the SC spectrum of the tellurite fiber pumped at 2 μm while the blue solid one shows the SC spectrum when pumped at 2.78 μm. The spectra of the input pulses at 2 μm and 2.78 μm are represented by the dash-dot magenta and the solid green curves, respectively. The dashed line in Fig. 1 shows the fiber’s ZDW. The inset in Fig. 1 shows the propagation loss of the tellurite fiber in the 0.5-5 μm wavelength range used in our simulation, which was derived from the loss of a tellurite fiber measured in the 0.5-4.5 μm wavelength range by NP Photonics [41]. When the tellurite fiber is pumped at 2 μm, which lies in the normal group velocity dispersion (GVD) region, a narrow and approximately symmetrical SC spectrum is obtained. The spectral evolution of the pulses in the fiber is plotted in Fig. 2(a). Because the pump wavelength is in the normal GVD region and also far from the ZDW, SPM is the dominant nonlinear process. The interaction of SPM and the normal GVD leads to the approximately symmetric spectrum. Since no spectral component can exceed the ZDW into the anomalous GVD regime at a pump peak power of 12 kW, significant spectral broadening doesn't occur in this case. When the tellurite fiber is pumped at 2.78 μm in the anomalous GVD region, the SC generation is dominated by soliton-related nonlinear effects that usually lead to significant spectral broadening. A SC with −40 dB bandwidth of nearly 2 μm is obtained as shown in Fig. 1. The spectral evolution of the pulses is plotted in Fig. 2(b). The spectrum of the 800 fs 2.78 μm pulses is substantially broadened, spanning over 1.5-3.5 μm in less than the beginning 10 cm fiber segment. As the pulses propagate in the remaining 50 cm fiber segment, the long wavelength wing of the SC spectrum shrinks slightly, which may be attributed to the periodic performance of solitons. Although SC generation in a conventional tellurite fiber pumped at 2.78 μm is much broader than that pumped at 2 μm, the bandwidth and flatness of the SC are still fairly far from those of a high-performance SC laser source.

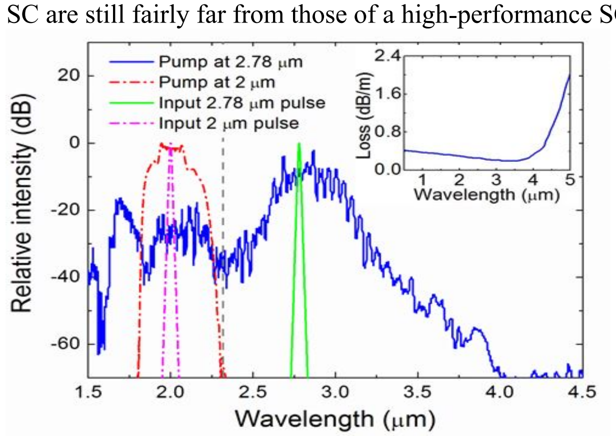

Fig. 1. The spectra of SCs generated in a 60 cm conventional tellurite fiber pumped by 12 kW 800 fs pulses at 2.78 μm (blue solid curve) and 2 μm (red dash-dot curve). The spectra of 2 μm and 2.78 μm input pulses are shown by the dash-dot magenta and the green solid curves, respectively. The grey dashed line indicates the ZDW of 2.32 μm. Inset: propagation loss of the single mode tellurite fiber in a wavelength range of 0.5-5 μm.

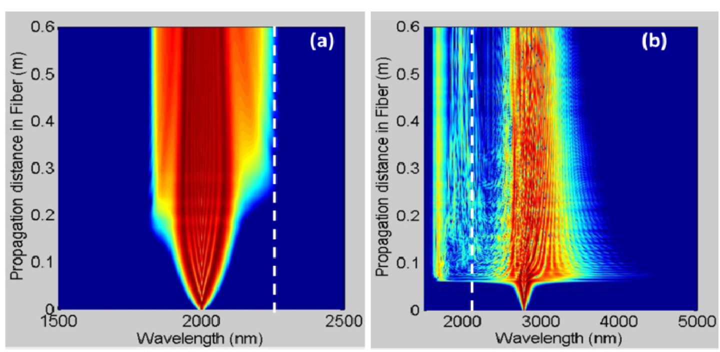

Fig. 2. The spectral evolution of (a) the 2 μm and (b) the 2.78 μm 12 kW 800 fs pulses propagating in a 60 cm tellurite fiber with a ZDW of 2.32 μm.

3.2 Design of a W-type dispersion-shifted tellurite fiber

It has been well recognized that an ultra-broad bandwidth, high flatness SC can be obtained when a nonlinear fiber is pumped at a wavelength close to its ZDW [42]. The ZDW of a conventional tellurite fiber is at 2.3 μm, but there is no readily available compact laser source around 2.3 μm. Therefore the most feasible approach is to shift the ZDW of an optical fiber to

#198149 - $15.00 USD Received 23 Sep 2013; revised 12 Nov 2013; accepted 12 Nov 2013; published 21 Nov 2013

the wavelength of a readily available ultrafast laser source by engineering the waveguide dispersion of the fiber. Tapered or microstructured tellurite fibers with ZDWs in the near IR have been fabricated and SC generation in these fibers has already been demonstrated. However, as discussed in Section 1, power scaling of these SC laser sources is constrained by the low power damage threshold of the small fiber core and their power proportions in the mid-IR region are limited by the near-IR pump wavelength. In order to obtain a high power, high flatness, ultra-broad bandwidth SC with a large mid-IR power proportion, we propose to fabricate a W-type tellurite fiber and pump it with our mode-locked Er^{3+}-doped ZBLAN fiber laser at 2.78 μm. The W-type fiber structure has been extensively used to shift the ZDW of silica fiber from 1.3 μm to 1.5 μm to suppress dispersion effects in long-haul optical communications. Therefore, it can be adopted to shift the ZDW of a tellurite fiber from 2.3 μm to a wavelength close to the operating wavelength of a mode-locked Er^{3+}-doped ZBLAN fiber laser. Moreover, since W-type fiber has a solid cladding, it will be more robust, easier to handle, and have better thermal tolerance than a microstructured tellurite fiber whose mechanical strength and thermal conductivity have been reduced largely due to air holes.

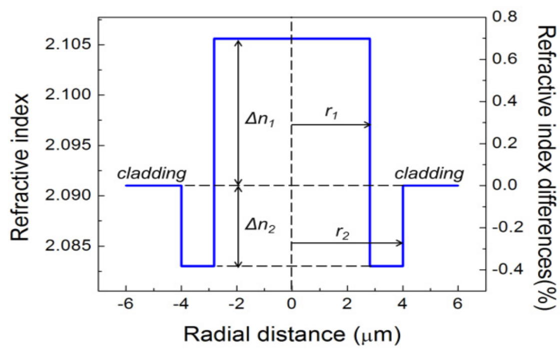

Fig. 3. The refractive index profile of the proposed W-type tellurite fiber (r_1 = 2.81 μm, r_2 = 4 μm, Δn_1 = 0.70%, and Δn_2 = 0.38%).

The index profile of the designed W-type tellurite fiber is shown in Fig. 3. The radius r_1 and r_2 are 2.81 μm and 4 μm, respectively. The refractive indices of the core and the cladding are 2.1056 and 2.091, respectively. The refractive index of the ring is set to be 2.083. The refractive index differences Δn_1 and Δn_2 are 0.70% and 0.38%, respectively. The guiding properties of this fiber were analyzed by calculating the guided modes using the fully vectorial modal solver of FIMMWAVE [43].

The waveguide dispersion and total dispersion of the designed W-type tellurite fiber are calculated and shown in Fig. 4. The waveguide dispersion (shown by the blue solid curve) is obtained by calculating the effective refractive index of the fundamental mode using FIMMWAVE software and then using the equation $D = -\frac{\lambda}{c}\frac{d^2 n}{d\lambda^2}$, where D represents the dispersion, λ, n, and c represent the wavelength, refractive index, and the speed of light, respectively. The material dispersion (shown by the red dash-dot curve) is calculated using Sellmeier equation with A = 2.5804773, B = 1.8635211, C = 6.3945516 × 10^{-2}, D = 2.4311168, E = 225 [16]. The total dispersion (shown by the magenta dotted curve) is the sum of the waveguide dispersion and the material dispersion. The grey dashed line represents the zero dispersion condition. We can see from Fig. 4 that the ZDW of the tellurite glass is at 2.3 μm and the ZDW of the W type tellurite fiber is shifted to 2.7 μm because of the negative waveguide dispersion. The insets (a) and (b) of Fig. 4 show the 3-D and 2-D intensity distribution of the fundamental mode of the W-type fiber at 2.78 μm, respectively. Clearly, the W-type fiber provides strictly single-mode guidance for the pump laser at 2.78 μm. Since

#198149 - $15.00 USD Received 23 Sep 2013; revised 12 Nov 2013; accepted 12 Nov 2013; published 21 Nov 2013

the waveguide dispersion can be engineered by tailoring the W-type fiber structure, it is found that the ZDW can be shifted to 2.9 μm when the ratio of r_1 to r_2 is increased to 1.88.

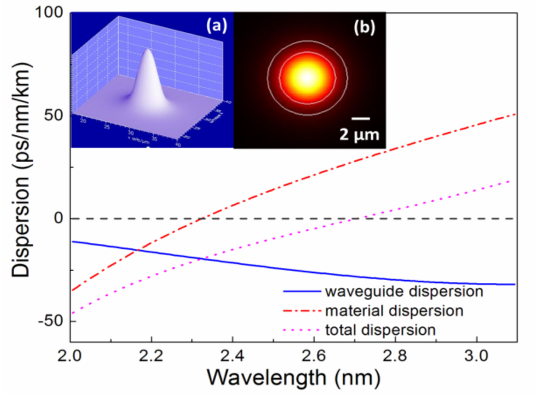

Fig. 4. Material dispersion (red dash-dot curve), waveguide dispersion (blue curve), and total chromatic dispersion (magenta dotted curve) of the designed W-type tellurite fiber in a wavelength range of 2-3.1 μm. The grey dashed line illustrates zero dispersion. Inset: (a) 3-D and (b) 2-D intensity distribution of the fundamental mode of the W-type tellurite fiber.

3.3 Mid-IR SC generation in different W-type tellurite fibers

It is well known that SC generation exhibits different features when the same pump pulse is launched into optical fibers with different ZDWs. It has also been demonstrated in Section 3.2 that the ZDW of a W-type tellurite fiber can be shifted from 2.3 μm to a longer wavelength by tailoring the W-type fiber structure. In this section, SC generation in W-type tellurite fibers with different ZDWs pumped at 2.78 μm is investigated.

Figure 5 shows the SC generated in 60 cm tellurite fibers with ZDWs of 2.32 μm (red solid curve), 2.7 μm (black dashed curve), and 2.9 μm (blue dash-dotted curve), respectively. The 2.78 μm pump pulses have a duration of 800 fs and a peak power of 12 kW. Clearly, SC generated in the tellurite fiber with a ZDW of 2.7 μm has the broadest spectrum and the best spectral flatness. Most importantly, the power proportion of output beyond 3 μm is also the largest (34.8%) among the three fibers. For the fiber with a ZDW of 2.32 μm, spectral extension to long wavelength is limited while spectral extension to short wavelength caused by dispersion wave generation is dominant. For the fiber with ZDW of 2.9 μm, however, the spectral broadening mainly relies on the soliton self-frequency shift and consequently results in significant spectral extension to long wavelength.

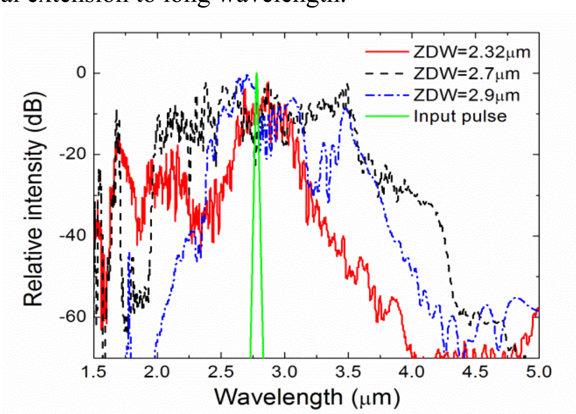

Fig. 5. The SC generated in 60 cm tellurite fibers with ZDWs of 2.32 μm (red solid curve), 2.7 μm (black dashed curve), and 2.9 μm (blue dash-dot curve), respectively. The 2.78 μm pump pulses (green solid curve) have a duration of 800 fs and a peak power of 12 kW.

#198149 - $15.00 USD Received 23 Sep 2013; revised 12 Nov 2013; accepted 12 Nov 2013; published 21 Nov 2013

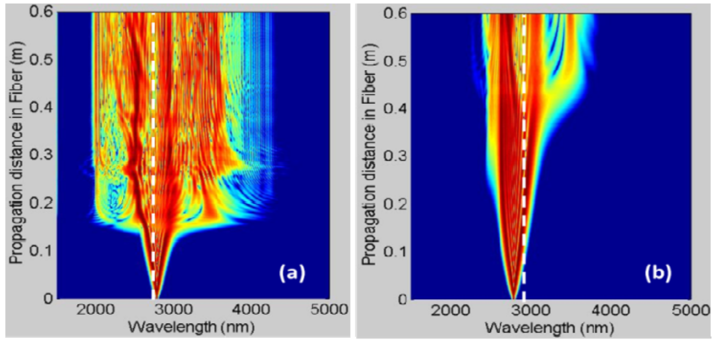

Fig. 6. The spectral evolutions of 2.78 μm pulses along the 60 cm tellurite fibers with ZDWs of (a) 2.7 μm and (b) 2.9 μm, respectively. (Pump pulse duration: 800 fs; peak power: 12 kW). The white dashed lines represent the ZDWs.

In order to thoroughly understand the underlying mechanisms behind different output spectra, spectral evolution in the three fibers were calculated and analyzed. Since the spectral evolution of the 2.78 μm pulses in the fiber with ZDW of 2.32 μm has already been plotted in Fig. 2(b), the spectral evolutions in the fibers with ZDW of 2.7 μm and 2.9 μm are plotted in Figs. 6(a) and 6(b), respectively. Clearly, symmetrical spectral broadening due to SPM is dominated at the initial stage of evolution in both cases. After this stage of symmetrical spectral broadening, the spectrum is significantly broadened by the development of distinct peaks on both the short- and long- wavelength sides of the input pumps because more nonlinear effects such as four-wave mixing, dispersion waves, Raman self-frequency shift, and cross phase modulation come into play. The abrupt short-wavelength edge of the SCs can be explained by the intrinsically narrowband nature of the dispersive wave resonance [42].

For the tellurite fiber with ZDW = 2.9 μm, although the pump wavelength lies in the normal GVD regime, the initial dynamics are dominated by the interaction of SPM and normal GVD, which can transfer energy to the spectral components in the anomalous GVD regime within a propagation distance of 20 cm because the pump wavelength is close to the ZDW. Further propagation of the pulses along the tellurite fiber results in significant spectral broadening due to soliton fission. Meanwhile, dispersion and Raman effects play roles in modifying the spectral structure. For tellurite fibers with ZDWs of 2.32 μm and 2.7 μm, the pump wavelength of 2.78 μm lies in the anomalous GVD region. In this case, spectral broadening is initially caused by the fission of higher-order solitons into red-shifted fundamental solitons and blue-shifted dispersive waves and consequently by self-frequency shift of these solitons and the soliton trapping effect between solitons and dispersive waves. Generally, the closer the pump wavelength to the ZDW of the fiber, the broader spectral width can be achieved and more distinct soliton peaks appear in the spectrum. The simulation results shown in Figs. 5 and 6 manifest this principle clearly. The SC generated in the fiber with ZDW of 2.7 μm has broader bandwidth than the fiber with ZDW of 2.32 μm because soliton fission in the fiber with ZDW of 2.7 μm is more significant. The magnitude of soliton fission can be evaluated by soliton order, which is defined by

$$N = (\gamma P_0 T_0^{\ 2} / |\beta_2|)^{1/2}, \tag{4}$$

where P_0 represents the input peak power and T_0 represents the input pulse duration. The soliton order of the fiber with ZDW = 2.7 μm is 68.2, which is much larger than the 22.1 for fiber with ZDW = 2.32 μm. Mathematically, the inverse dependence of soliton order N on the squared dispersion $|\beta_2|^{1/2}$ also indicates the advantage of a pump wavelength closer to the ZDW. In addition, the > 3 μm power proportion for the fiber with ZDW of 2.7 μm is also larger than that of the fiber with ZDW = 2.32 μm.

From the viewpoint of practical application, the power proportion of SC light beyond 3 μm and the IR edge (defined by the longest wavelength with relative intensity of −40 dB) are two critical features of high power mid-IR SC laser sources. Because the dependence of these two features on the peak power and pulse duration of the pump pulse is essential for the development of high power mid-IR SC laser sources, the two features of SC generated in a 60 cm W-type tellurite fiber with ZDW of 2.7 μm pumped by 2.78 μm pulses with different peak powers and pulse durations are calculated and analyzed. The power proportion of the light with wavelength longer than 3 μm and the long wavelength edge of the SC as a function of the peak power of the 1.6 ps pump pulses were calculated and are shown in Fig. 7 by the black and the blue curves, respectively. Obviously, both the power proportion beyond 3 μm and long wavelength edge increase significantly with the increased peak power when the peak power is less than 10 kW. When the peak power is higher than 10 kW, the power proportion of the light with wavelength beyond 3 μm increases slightly with the increased peak power. Similarly, the long wavelength edge only increases from 4.27 μm to 4.65 μm as the peak power increases from 10 kW to 30 kW. The increases of the mid-IR power proportion and the long wavelength edge with the increased peak power from 1 kW to 10 kW are due to the strong Raman scattering assisted soliton self-frequency shifting. As the peak power is larger than 10 kW, the increases of both features become slight because the long wavelength edge of the SC approaches to the IR edge of the tellurite fiber and the loss greatly increases with increasing wavelength as shown by the inset in Fig. 1.

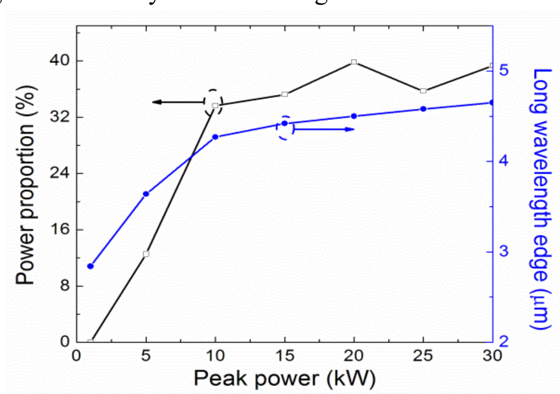

Fig. 7. Power proportion of the laser with wavelength > 3 μm (black curve) and the long wavelength edge (blue curve) of the SC as a function of the peak power of 1.6 ps pump pulses.

The power proportion of the light with wavelength longer than 3 μm and the long wavelength edge of the SC as a function of the pulse duration of the input pulse are shown in Fig. 8. The peak power of the 2.78 μm pulse is fixed to be 12 kW. The power proportion beyond 3 μm is almost the same (34%) for pulse durations from 200 fs to 3 ps. The long wavelength edge, however, increases greatly with the increased pulse duration from 200 fs to 1.6 ps. This is because the soliton order monotonically increases with the pulse duration as shown by Eq. (4). There is almost no change as the pulse duration increases from 1.6 ps to 3.2 ps because the bandwidth of the SC generated by the 1.6 ps pump pulses has already arrived at a bandwidth limited by the IR edge of the tellurite fiber. Based on Figs. 7 and 8, we can draw the conclusion that an ultrafast fiber laser at 2.78 μm with pulse duration of 1.6 ps and peak power of 12 kW is a suitable pump source for SC generation in W-type tellurite fiber.

3.4 Power scalability of tellurite fiber SC laser source

Although tellurite fiber SC laser sources have been reported by several groups, their output powers are at a level of tens of mWs [17], which is much lower than the required power for some specific applications, where high power (> 10 W) mid-IR SC with high spectral brightness are highly demanded. In contrast to tapered and microstructured fibers that have been used for mid-IR SC generation by other research groups [17–26], our approach of using

#198149 - $15.00 USD Received 23 Sep 2013; revised 12 Nov 2013; accepted 12 Nov 2013; published 21 Nov 2013

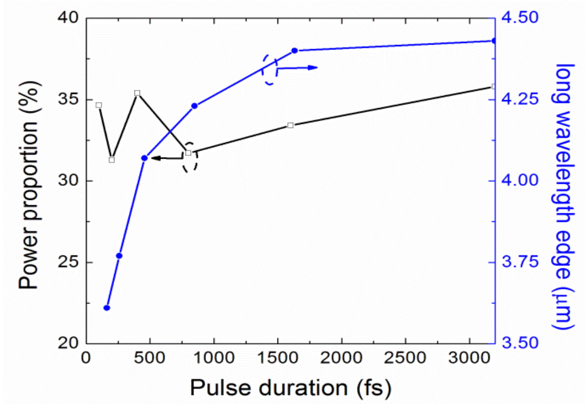

Fig. 8. Proportion of SC laser power with wavelength > 3 μm (black curve) and the long wavelength edge (blue curve) of the SC as a function of the input pulse duration of a pump pulse with peak pump of 12 kW.

W-type fiber has substantial potential for power scaling because this fiber can sustain much higher pump power due to the large core size and solid cladding. In order to shift the ZDW of a tellurite fiber to 2 μm or 1.5 μm where ultrafast silica fiber lasers are readily available, the core diameters of these microstructured or tapered fibers have been shrunk to ~3 μm or less [17–26] and the effective core areas are less than 6 μm^2. W-type fiber with ZDW = 2.7 μm, however, has a core size of 8 μm and an effective core area of nearly 50 μm^2. Therefore, W-type tellurite fiber can handle much higher pump power than these microstructured or tapered fibers. Provided that the damage threshold of tellurite glass is 15-20 GW/cm^2 [35], the sustainable pump power as a function of the effective core area is plotted in Fig. 9. W-type fiber can handle more than 7 kW pump power, which is more than 8 times larger than those of the microstructured or tapered fibers labeled by green dots [17–26]. Therefore, W-type tellurite fiber is a promising candidate for high power mid-IR SC generation. Assuming an optical-to-optical conversion efficiency of the SC of around 60% [44], the attainable output power of a mid-IR SC laser source based on W-type tellurite fiber can be larger than 4 kW. However, an SC fiber is often damaged in practice by heat induced effects rather than optical damage of the fiber glass. Since a 10 W SC laser source has been demonstrated in a ZBLAN fiber [12], it is quite feasible to develop a 100 W or higher power mid-IR SC laser source with a W-type tellurite fiber because tellurite glass [15] has better mechanical strength, higher resistance to thermal effects, higher nonlinearity, and higher damage threshold than ZBLAN glass [11].

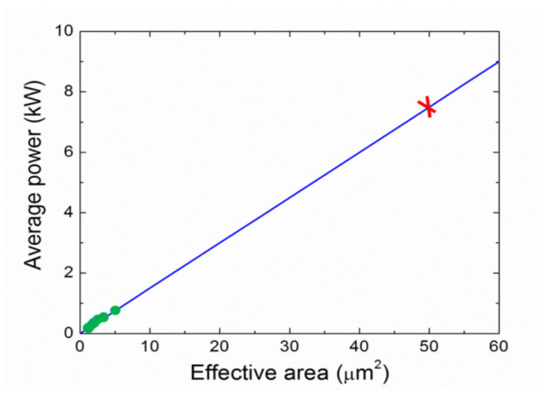

Fig. 9. Sustainable power as a function of effective core area of the tellurite fiber. The red cross represents the handling power of the proposed W-type tellurite fiber. The green dots represent the handling power of the fibers used in previous works.

4. Mid-IR SC generation in chalcogenide fiber

Chalcogenide glasses are the only class of amorphous materials to exhibit high transparency over the entire mid-IR region including the two atmospheric windows at 3-5 and 8-12 μm. In addition to their optical properties, these glasses are thermodynamically stable and show excellent rheological properties which allow them to be drawn into fibers or molded into complex lenses. The width of the optical window of chalcogenide fibers is directly dependent on the phonon energy of the glass matrix and can be tuned to expand beyond 10 μm for Se glass [45]. Therefore, chalcogenide fiber can be used to obtain an SC laser source beyond 5 μm where the propagation loss of ZBLAN and tellurite fibers becomes tremendously large. Moreover, chalcogenide glass has a very high nonlinearity ($n_2 = 1.5 \times 10^{-17}$ m^2/W [29]), which is hundreds of times higher than that of silica. Such high nonlinearity allows very low threshold SC generation in chalcogenide nanofibers (peak power: 7.8W, pulse energy: 2.2 pJ) [30]. All these attractive properties have made As_2Se_3 chalcogenide fiber a promising candidate for a mid-IR SC spanning over the two atmospheric windows. However, the ZDW of a conventional As_2Se_3 chalcogenide fiber is ~5 μm [35], which is much longer than the wavelengths of the readily available pump laser sources and our 2.78 μm mode-locked Er^{3+}-ZBLAN fiber laser. As discussed in Section 3, high flatness, an ultrabroad bandwidth SC laser source can be easily obtained provided that the pump wavelength is close to the ZDW of the nonlinear fiber. Therefore, various techniques to shift the ZDW of chalcogenide fiber to a short wavelength including microstructured [32,45], fiber tapering [34], or the combination of both have been used in chalcogenide fibers for efficient SC generation. Here, we propose to fabricate an As_2Se_3 PCF and pump it with our mode-locked Er^{3+}-doped ZBLAN fiber laser at 2.78 μm to generate mid-IR SC that extends beyond 10 μm. We chose the PCF technology because the ZDW of a PCF can be engineered over a very wide wavelength range compared to that of a tapered fiber.

4.1 Design of chalcogenide PCF

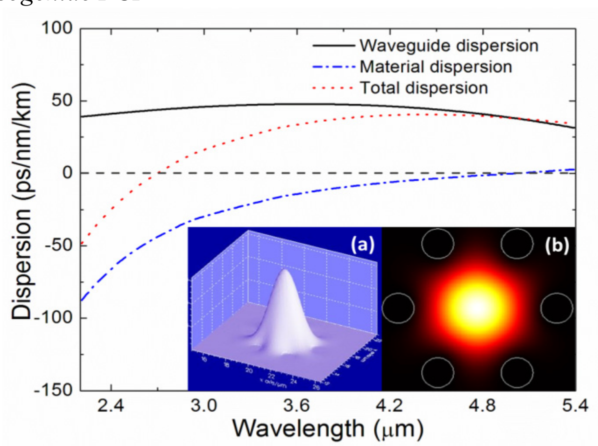

Fig. 10. Chromatic dispersion of the designed As_2Se_3 PCF as a function of wavelength. Black solid curve: waveguide dispersion; blue dash-dot curve: material dispersion; red dotted curve: total chromatic dispersion. The grey dashed line represents zero dispersion. Inset: (a) 3-D and (b) 2-D near-field distribution of the fundamental mode of the designed As_2Se_3 PCF (r = 0.61 μm, Λ = 3 μm).

In order to shift the ZDW of a chalcogenide fiber to the wavelength of our mode-locked Er^{3+}-doped ZBLAN fiber laser, an As_2Se_3 PCF as shown in Fig. 10(b) was designed. The core of the As_2Se_3 PCF was created by introducing a defect in the air-hole array, in which the air-hole radius and the pitch of the array are 0.61 μm and 3 μm, respectively. The refractive index of the background is set to be 2.78. The material, waveguide and total dispersions of the PCF are shown in Fig. 10. The waveguide and total dispersion were calculated using the same method

#198149 - $15.00 USD Received 23 Sep 2013; revised 12 Nov 2013; accepted 12 Nov 2013; published 21 Nov 2013

as for the tellurite fiber. The material dispersion is obtained estimated using the Sellmeier equation with A = 2.6, B = 1.759, C = 2.756 × 10^{-2}, D = 0.02792, and E = 101.6683 [35]. Because of the large positive waveguide dispersion of the PCF, the ZDW of the As_2Se_3 PCF is shifted to 2.7 μm. The insets (a) and (b) in Fig. 10 show the 3-D and 2-D intensity distributions of the fundamental mode at the pump wavelength of 2.78 μm, respectively. Clearly, this PCF exhibits excellent guiding capability for a single-mode pump laser at 2.78 μm because the laser field concentrates in the core area and thus enables considerable nonlinear interaction.

4.2 Mid-IR SC generation in the As_2Se_3 PCF

In the last section, we have demonstrated that the ZDW of a chalcogenide PCF can be shifted from 5 μm to 2.7 μm. In this section, SC generations in the designed As_2Se_3 PCF pumped at 2.78 μm are numerically studied. In our simulation, we assumed the same Raman gain of As_2Se_3 glass as used in [38]. The propagation loss of the As_2Se_3 chalcogenide fiber shown in the inset of Fig. 11(a) was determined from the loss of a Coractive As_2Se_3 fiber [46]. The output spectrum of 800 fs pulses with peak power of 1 kW propagating through a 10 cm As_2Se_3 fiber is shown in Fig. 11(a). The spectral evolution of the pulses along the As_2Se_3 fiber was calculated and is shown in Fig. 11(b). Similar to a general spectral evolution of pulses with a wavelength in the anomalous GVD regime and close to the ZDW of the nonlinear fiber, the initial stage of spectral evolution exhibits approximately symmetrical spectral broadening, which occurs in the beginning 2.5 cm fiber segment. After a propagation of about 3 cm, the spectrum of the pulses experiences significant spectral broadening with the development of distinct spectral peaks on both the short- and long-wavelength sides of the injected pump due to soliton fission and the Raman self-frequency shift of ejected constituent fundamental solitons. The spectrum of the pulses spans over 2-12 μm after a propagation of 4 cm. Further propagation of the pulses along the As_2Se_3 fiber results in increased flatness of the SC. Clearly, high flatness mid-IR SC spanning over two atmospheric windows can be achieved by pumping an As_2Se_3 PCF with an ultrafast fiber laser at 3 μm.

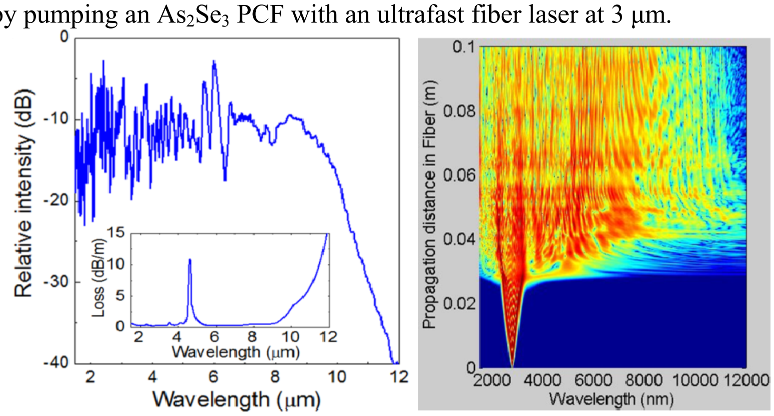

Fig. 11. (a) Output spectrum of the SC generated in a 10 cm As_2Se_3 PCF with 2.7 μm ZDW pumped at 2.78 μm. Inset: Propagation loss of a single-mode As_2Se_3 fiber in a wavelength range of 1.5-12 μm. (b) The SC spectral evolution in the 10 cm As_2Se_3 PCF. (Input pulse duration: 800 fs; peak power: 1 kW).

In order to guide the development of mid-IR SC sources and determine the requirement of the mode-locked fiber laser at 3 μm, the dependence of power proportion of the light beyond 3 μm and the long wavelength edge of the SC on the input pulse duration and peak power was studied. Figure 12 shows the proportion of the light power beyond 3 μm and the long wavelength edge of the SC as a function of the pulse duration. Both the power proportion and long wavelength edge increase with the increased pulse duration. As the pulse duration becomes greater than 400 fs, the increase of the mid-IR power proportion and long

#198149 - $15.00 USD Received 23 Sep 2013; revised 12 Nov 2013; accepted 12 Nov 2013; published 21 Nov 2013

wavelength edge with the increased pulse duration becomes modest. This we attribute to the greatly increased loss of the As_2Se_3 chalcogenide fiber at wavelengths longer than 10 μm as shown in the inset of Fig. 11(a). Figure 13 shows the power proportion of the light beyond 3 μm and the long wavelength edge of the SC as a function of the peak power of 800 fs pulses. Both the power proportion and long wavelength edge increase almost linearly with the peak power. The results shown in Fig. 12 and Fig. 13 tell us that a mid-IR SC with a power proportion of the light beyond 3 μm > 80% and the long wavelength edge up to ~12 μm can be achieved by pumping a 10 cm As_2Se_3 PCF with 2.78 μm 800 fs pulses with peak power of 1 kW.

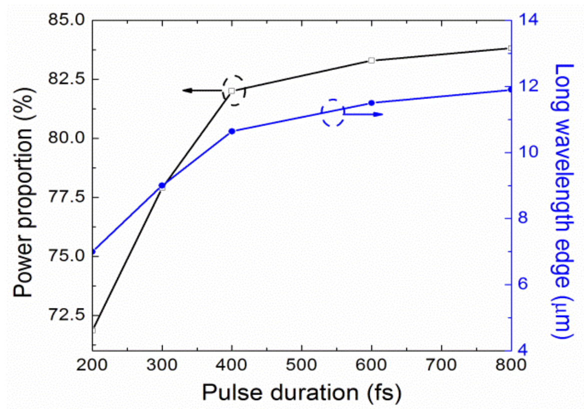

Fig. 12. Power proportion of the light beyond 3 μm contained in the SC (black curve) and the long wavelength edge (blue curve) of the SC as a function of the input pulse duration. (Peak power: 1 kW; fiber length: 10cm).

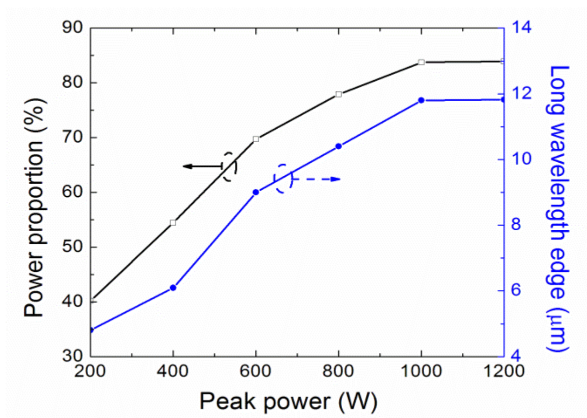

Fig. 13. Power proportion of the light beyond 3 μm contained in the SC (black curve) and the long wavelength edge (blue curve) of the SC as a function of the input peak power. (Pulse duration: 800 fs; fiber length: 10 cm).

4.3 Power scalability of chalcogenide fiber SC laser source

Compared to a standard step-index fiber, a PCF generally can sustain a lower power due to its small core size, low robustness, and low heat dissipation ability. In addition, chalcogenide glass has a much lower damage threshold (~1 GW/cm^2 [47]) than tellurite glass. Therefore, it is challenging to achieve a high power, high flatness, ultrabroad mid-IR SC laser source using a chalcogenide PCF. Special protection and heat dissipation management have to be employed for a chalcogenide fiber SC laser source. Here, we just discuss the power scalability of the chalcogenide fiber SC laser source by comparing the sustainable pump power for different chalcogenide PCFs and those chalcogenide fibers used in previous reports. Our designed As_2Se_3 PCF not only has the advantage of easy fabrication because it is relatively easier to shift the ZDW from 5 μm to 2.7 μm than to 1.9 μm or 1.5 μm by use of microstructured fiber construction, but also bring the benefit of a large effective core area. The effective area of the designed As_2Se_3 chalcogenide PCF shown in Fig. 10(b) is 14.38 μm^2, which is much larger than those of As_2Se_3 chalcogenide PCFs with ZDW in the near IR. For instance, As_2Se_3 chalcogenide PCFs with ZDW of 1.9 μm and 1.45 μm can be designed by keeping the air hole radius constant at 0.61 μm and adjusting the ratio of the air hole radius and the pitch of the PCF (r/Λ) to be 0.347 and 0.484, respectively. The chromatic dispersions of the two PCFs are shown in Fig. 14. The profiles of the guided fundamental modes at 2 μm and 1.5 μm are plotted and shown in Figs. 14(a) and 14(b), respectively. Their effective core areas are only 3.313 μm^2 and 0.977 μm^2, respectively. The maximum sustainable power of the three PCFs are predicted and shown in Fig. 15 by red crosses. The sustainable pump power of the PCFs with ZDW of 2.7 μm is about 144 W, which is much larger than 33 W and 9.8 W for these two PCFs with ZDW in the near-IR. Assuming that an optical-to-optical conversion efficiency of 60% [48] can be obtained, the maximum attainable output power of an As_2Se_3 chalcogenide PCF SC laser source can be 86.3 W. The sustainable pump powers of the chalcogenide fibers used in previous reports [32,34,48,49] are also shown in Fig. 15, indicated by the green dots. Clearly, the proposed As_2Se_3 SC laser source has the largest attainable output power.

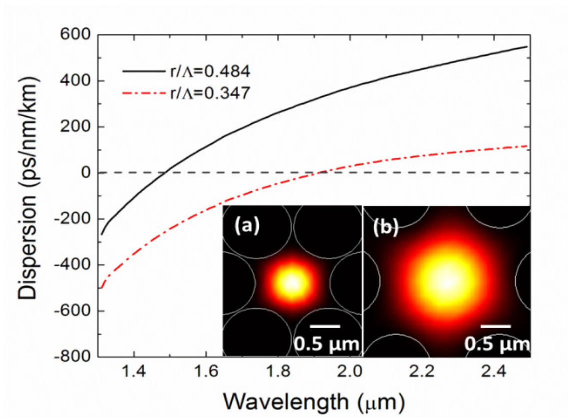

Fig. 14. Chromatic dispersion of two As_2Se_3 PCFs with r/Λ = 0.484 (black solid curve) and 0.347 (red dash-dot curve) as a function of the wavelength. Inset: the fundamental mode profiles of the PCF with r/Λ = 0.484 (a) and 0.347 (b) at the pump wavelengths of 1.5 μm and 2 μm, respectively. The dashed line represents the zero dispersion.

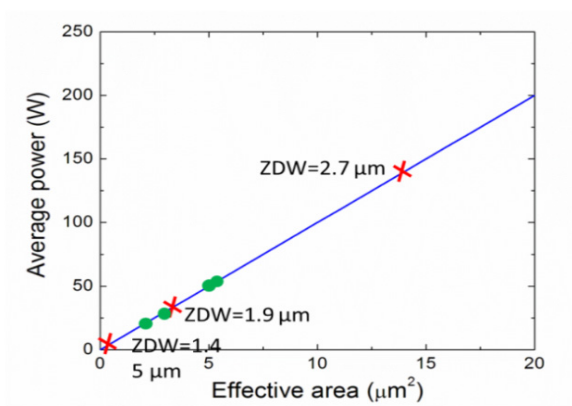

Fig. 15. Sustainable power as a function of effective area of the chalcogenide PCF. The marked red crosses represent the handling power of the PCFs with different ZDWs by assuming an optical-to-optical conversion efficiency of 60% [48]. The green dots represent the handling powers of these chalcogenide fibers used in previous works.

Although chalcogenide fiber has the largest nonlinearity and the broadest mid-IR transparent window among current available optical fibers, existing chalcogenide fiber SC laser sources with moderate spectral bandwidth and low mid-IR spectral power density haven't shown significant promise so far. Pumping an As_2Se_3 PCF with a mode-locked ZBLAN fiber laser at 3 μm is emerging as promising approach to achieve a mid-IR SC laser source spanning over the range 2-12 μm.

5. Conclusion

In conclusion, we have demonstrated that mid-IR SC can be generated in dispersion engineered W-type tellurite fiber and As_2Se_3 chalcogenide PCF when they are pumped with ultrafast fiber lasers at 2.78 μm. The power proportion of the light beyond 3 μm and the long wavelength edge of the mid-IR SC as a function of the peak power and pulse duration of the input pulse have been studied. Our simulation shows that mid-IR SC with a long wavelength edge of 4.65 μm and ~40% power proportion beyond 3 μm can be generated in a W-type tellurite fiber pumped by a 1.6 ps pulsed laser with peak power of 30 kW. When a chalcogenide PCF is pumped by 1 kW 800 fs pulses, a mid-IR SC with its long wavelength edge up to 12 μm and with > 80% mid-IR power proportion can be achieved. Most importantly, compared to microstructured or tapered tellurite and chalcogenide fibers used in previous works, the attainable output power of the W-type tellurite fiber can be increased by one order of magnitude and that of the As_2Se_3 chalcogenide PCF can be increased by three times. Our study demonstrates that W-type tellurite fiber is a promising candidate for 10W-100W mid-IR SC laser sources in the 3-5 atmospheric window, while As_2Se_3 PCF has the potential to generate a mid-IR SC covering the 3-5 μm and 8-10 μm atmospheric windows and most molecular "fingerprint" spectral regions.

Acknowledgments

This work was supported by International Cooperation Program of Ministry of Science and Technology (MOST) and National Science Foundation of China (61138004) and partially supported by National Science Foundation Engineering Research Center for Integrated Access Networks (Grant #EEC-0812072) and the Photonics Initiative of the University of Arizona (TRIF). Chen Wei and Feng Song would like to thank Chinese Scholarship Council for financial support. The authors would like to thank Qiang Fang for helpful discussion.